CHANSON, H., YASUDA, Y., and OHTSU, I. (2002). "Flow Resistance in Skimming Flows and its Modelling." *Can Jl of Civ. Eng.*, Vol. 29, No. 6, pp. 809-819 (ISSN 0315-1468).

Flow Resistance in Skimming Flows in Stepped Spillways and its Modelling

H. Chanson (1), Y. Yasuda (2), and I. Ohtsu (3)

(1) Reader, Dept of Civil Engineering, The University of Queensland, Brisbane QLD 4072, Australia

Ph.: (61 7) 33 65 35 16 - Fax: (61 7) 33 65 45 99 - Email: h.chanson@uq.edu.au

(2) Associate Professor, Dept of Civil Engineering, College of Science and Technology, Nihon University, Tokyo 101-8303, Japan

(3) Professor, Dept of Civil Engineering, College of Science and Technology, Nihon University, Tokyo 101-8303, Japan

Abstract

Dams and weirs must be equipped with adequate flood release facilities for a safe dissipation of the kinetic energy of the flow. With stepped spillway design, it is essential to predict accurately the flow resistance contribution of the steps. The authors investigate the flow resistance of skimming flows and associated form losses. Recent laboratory experiments were systematically performed with channel slopes ranging from 5.7º up to 55º and they are compared with existing laboratory and prototype data. The results provide a better understanding of the basic flow patterns and flow resistance mechanisms. They emphasise that form loss is dominant. Simple analytical models provide a reasonable order of magnitude of the pseudo-boundary shear stress and of the recirculation cavity ejection frequency. Altogether more than 38 model studies and 4 prototype investigations (totalising more than 700 data points) are re-analysed.

Keywords : stepped spillway, flow resistance, skimming flow, form drag, physical and analytical modelling

Résumé

Les barrages et ouvrages de retenues déau doivent être équippés de systèmes d'évacuations des eaux de crues, permettant une dissipation efficace de l'énergie cinétique de l'écoulement. Dans le cas d'évacuateurs de crues en marches d'escalier, il est particulièrement important d'estimer correctement les forces de frottement dues aux marches. On étudie, particulièrement, la résistance de frottement des écoulements extrèmement turbulents (*skimming flows*) et leur résistance de forme. Des essais en laboratoires ont été conduits systématiquement pour des pentes comprises entre 5.7 et 55 degrés, et les données expérimentales sont comparées avec des études antérieures. Les résultats permettent de comprendre mieux les caractéristiques des écoulements et les mécanismes de bases de perte de charge. Ils démontrent, en particulier, l'importance de la résistance de forme (*form drag*). On présente, de plus, de simples modèles analytiques fournissant une estimation raisonnable de la contrainte équivalent de paroi (*pseudo boundary shear stress*) et de la fréquence d'éjection des zones de recirculation. Au total, plus de 38 études en laboratoire et 4 études sur prototypes (regroupant plus de 700 points de mesure) sont ré-analysées.

Mots-clés: évacuateur de crues en marches d'escalier, perte de charge, écoulement extrèmement turbulent, résistance de forme, modèlisation physique et analytique.

Introduction

During large rainfall events, flood waters rush through, above and beside man-made dams. Significant damage may occur if the energy of the flow, especially its kinetic energy, is not dissipated safely. One type of flood release facility is the stepped spillway. It is characterised by significant flow resistance and associated energy dissipation caused by the steps. The design yields smaller, more economical dissipation structures at the downstream end of the chute. The world's oldest stepped spillway is presumably the overflow stepped weir in Akarnania, Greece, built around B.C. 1,300. The weir, 10.5-m high with a 25-m long crest, was equipped with a stepped overflow (Knauss 1995, Chanson 2000). The downstream slope is stepped (14 steps) with masonry rubble set in mortar. The mean slope is about 45º, varying from 39º down to 73º and the step height ranges from 0.6 to 0.9-m. The stepped weir was used for several centuries. It is still standing and flash floods spill over the stepped chute.

The recent regain of interest in stepped spillways has been associated with the development of new construction materials (e.g. roller compacted concrete) and design techniques (e.g. overflow protection systems for embankments) (e.g. Chanson 1995, Nihon University 1998). Although modern roller compacted concrete (RCC) stepped spillways are designed for a skimming flow regime (Fig. 1), there is some controversy on an accurate estimate of the flow resistance. Model and prototype data exhibit little correlation, with flow resistance data scattered over three orders of magnitude (e.g. Nihon University 1998, Chanson et al. 2000) (Fig. 2).

In the present paper, the authors investigate the flow resistance in skimming flows. New experiments were performed systematically with channel slopes ranging from 5.7 up to 55º. Basic flow patterns are presented and the experimental results are compared with existing data: i.e., over 38 model and 4 prototype studies are re-analysed including more than 700 data points. It is the purpose of this paper to assess critically the overall state of this field and to present new conclusions valid for both flat ($\theta < 20º$) and steep ($\theta > 20º$) spillways with skimming flows.

CHANSON, H., YASUDA, Y., and OHTSU, I. (2002). "Flow Resistance in Skimming Flows and its Modelling." *Can Jl of Civ. Eng.*, Vol. 29, No. 6, pp. 809-819 (ISSN 0315-1468).

Basic equations

While the flow resistance on smooth-invert chutes is primarily skin friction, skimming flows over stepped chutes are characterised by significant form losses. The water skims over the step edges with formation of recirculating vortices between the main flow and the step corners (Fig. 1). In *uniform equilibrium flows*, the momentum principle states that the boundary friction force equals exactly the gravity force component in the flow direction : i.e., the weight-of-water component acting parallel to the pseudo-bottom formed by the step edges. It yields:

$$\tau_o * P_w = \rho_w * g * A_w * \sin\theta \qquad [1]$$

where τ_o is the average shear stress between the skimming flow and the recirculating fluid underneath, P_w is the wetted perimeter, ρ_w is the water density, g is the gravity constant, A_w is the water flow cross-sectional area and θ is the mean bed inclination angle. For a wide channel, Equation (1) becomes :

$$\tau_o = \left(\int_{y=0}^{y=Y_{90}} \rho_w * (1 - C) * dy \right) * g * \sin\theta \qquad [2a]$$

where C is the void fraction, also called air concentration, defined as the volume of air per unit volume of air and water, and Y_{90} is the distance normal to the pseudo-bottom where C = 90%.

Kazemipour and Apelt (1983) stressed that to try to account for the form losses with a Gauckler-Manning or Darcy-Weisbach formula is unsatisfactory. Nevertheless the Darcy-Weisbach formula is used for this study of skimming flows because it facilitates a comparison between smooth-invert and stepped chute flows. Further the drag coefficient of uniformly-spaced roughness (e.g. steps) is proportional to the Darcy coefficient (Schlichting 1979). By analogy with clear-water open channel flows, the average boundary shear stress may be expressed in terms of the Darcy friction factor as:

$$\tau_o = \frac{f_e}{8} * \rho_w * V^2 \qquad [3]$$

where f_e is the Darcy friction factor of the air-water flow and V is the mean flow velocity (or equivalent clear-water flow velocity). By continuity, V equals :

$$V = \frac{q_w}{\int_{y=0}^{y=Y_{90}} (1 - C) * dy} \qquad [4]$$

In dimensionless terms, the momentum equation at uniform equilibrium in a wide channel yields :

[2b] $$\frac{\tau_o}{\frac{1}{8} * \rho_w * V^2} = \frac{8 * g}{q_w^2} * \left(\int_{y=0}^{y=Y_{90}} (1 - C) * dy \right)^3 * \sin\theta$$

In *gradually-varied flows*, the friction factor must be deduced from the friction slope S_f. The friction slope is the slope of the total head line (Henderson 1966, Chanson 1999). For a wide channel, it yields:

[5] $$\frac{\tau_o}{\frac{1}{8} * \rho_w * V^2} = \frac{8 * g}{q_w^2} * \left(\int_{y=0}^{y=Y_{90}} (1 - C) * dy \right)^3 * S_f$$

Free-surface aeration is always substantial in prototype skimming flows and its effects must not be neglected. Downstream of the inception point of free-surface aeration, the distribution of air concentration may be described by a diffusion model :

[6] $$C = 1 - \tanh^2\left(K' - \frac{y}{2*D'*Y_{90}}\right)$$

where tanh is the hyperbolic tangent function and y is the distance normal to the pseudo-bottom formed by the step edges, D' is a dimensionless turbulent diffusivity and K' is an integration constant (Chanson 1997). D' and K' are functions of the mean air content C_{mean} only and they may be estimated as:

[7] $$D' = \frac{0.848*C_{mean} - 0.00302}{1 + 1.1375*C_{mean} - 2.2925*C_{mean}^2}$$

[8] $$K' = \tanh^{-1}(\sqrt{0.1}) + \frac{0.5}{D'}$$

for $C_{mean} < 0.7$. Equation (6) compares favourably with stepped chute data obtained in models and prototype (Baker 1994, Ruff and Frizell 1994, Chamani and Rajaratnam 1999, Matos et al. 1999, Chanson and Toombes 2001a) (Fig. 3).

Flow resistance in skimming flows

Recent laboratory studies of stepped channels provided significant contributions to the understanding of stepped channel flows (e.g. BaCaRa 1991, Ohtsu and Yasuda 1997). Dynamic similarity of skimming flows is, however, complex because of the role of the steps in enhancing turbulent dissipation and free-surface aeration. For uniform equilibrium flows (i.e. normal flows) down a prismatic rectangular channel with horizontal steps, a dominant flow feature is the momentum exchange between the free-stream and the cavity flow within the steps (Fig. 1). A complete dimensional analysis yields :

$$[9] \quad F\left(\frac{V}{\sqrt{g * d}} ; \rho_w \frac{V * d}{\mu_w} ; \frac{g * \mu_w^4}{\rho_w * \sigma^3} ; C_{mean} ; \frac{d}{h} ; \frac{W}{h} ; \theta ; \frac{k_s'}{h}\right) = 0$$

where V and d are the mean flow velocity and flow depth at uniform equilibrium flow conditions, W the channel width, h is the step height, k_s' the skin roughness height, g the gravity acceleration, μ_w and ρ_w the dynamic viscosity and density of water respectively and σ the surface tension. For air-water flows, the equivalent clear water depth is defined as :

$$[10] \quad d = \int_{y=0}^{y=Y_{90}} (1 - C) * dy$$

From left to right, the dimensionless terms in Equation (9) are Froude, Reynolds and Morton numbers, the amount of entrained air, and the last four characterise the cavity shape and the skin friction effects on the cavity walls.

Equation (9) illustrates that a Froude similitude with geometric similarity and same fluids in model and prototype does not describe the complexity of stepped spillway flows. BaCaRa (1991) described a systematic laboratory investigation of the M'Bali dam spillway with model scales of 1/10, 1/21.3, 1/25 and 1/42.7. For the scales 1/25 and 1/42.7, the flow resistance was improperly reproduced with a Froude similitude. Further studies demonstrated that air entrainment is poorly reproduced on small-size scale models (Esslingen 1984, Chanson 1997). The latter recommended the use of model scales ranging from 1/1 to 1/10 to avoid significant scale effects (Chanson 1997, p. 236).

New experimental study

A systematic study of stepped spillway flows was undertaken at Nihon University (Yasuda and Ohtsu 1999). Experiments were performed in four 0.4-m wide stepped channels with bottom slopes of 5.7º, 11.3º, 19º, 30º and 55º, step heights ranging from 0.002 to 0.08 m and flow rates per unit width between 0.008 and 0.08 m^2/s. Each channel was followed by a horizontal stilling basin. Clear-water depths were recorded with a point gauge. Pressure and velocity in clear-water flows were measured with a Pitot tube. Void fractions were recorded with an optical fibre probe (single-tip). The skimming flow depth was measured by two methods : the clear-water flow depth deduced from void fraction profiles (Eq. (10)) and an indirect method based upon the water depth measurement in the stilling basin. In the stilling basin, the momentum equation across the jump yields :

$$[11] \quad \rho_w * q_w * (V_2 - V_1) = \frac{1}{2} * P_{bottom} * d_1 - \frac{1}{2} * \rho_w * g * d_2^2$$

where P_{bottom} is the invert pressure upstream of the hydraulic jump, d_1 and V_1 are the supercritical flow depth and velocity upstream of the hydraulic jump, and d_2 and V_2 are the flow depth and velocity downstream of the jump. At the chute toe, the energy equation implies that the residual head equals :

$$[12] \quad H_{res} = d * \cos\theta + \frac{V^2}{2 * g} = C_P * d_1 + \frac{V_1^2}{2 * g}$$

where d and V are the flow depth and velocity at the end of the stepped chute, and C_P is a pressure correction coefficient defined as :

$$C_P = \frac{1}{\rho_w * g * q_w * d_1} * \int_{y=0}^{y=d_1} (P + \rho_w * g * y) * v * dy$$

Pressure and velocity distributions upstream of the jump were measured in-situ with Pitot tube and pressure tappings. The data showed that C_P was significantly larger than unity. Comparison between clear-water flow depths deduced from the optical fibre probe (Eq. (10)) and indirect supercritical depth (Eq. (12)) showed agreement between the two methods within 10% and no significant trends between results of clear-water depths obtained by the different methods.

Additional experiments were conducted for two intermediate slopes (θ = 16 and 22°) and large step height (h = 0.1 m & 0.05 m) at the University of Queensland (Chanson and Toombes 2001a). This study was focused on the basic air-water flow properties and cavity recirculation processes.

Data analysis

The experimental data were analysed using Equations (2) and (5) for uniform equilibrium and gradually-varied flows respectively. They are compared with the re-analysis of over 40 model and prototype studies using the same equations. Some studies conducted detailed air-water flow measurements (e.g. void fraction distributions), while others attempted to record a pseudo-water depth (Table 1). Results derived from air-water flow data provide genuine estimate of the dimensionless boundary shear stress, herein denoted f_e. Estimates derived from Equation (12) are denoted f_p. Results based upon pseudo-water depth give a rough, less accurate estimate that is denoted f_w.

The combined analysis (over 700 data points) shows that the flow resistance is larger on stepped chutes than on smooth channels, but the steep stepped chute data show very little correlation (Fig. 2). The study highlights further the lack of uniformity in the experimental procedure and data processing. Many studies gave incomplete experimental information with uncertainties of up to 200%.

A conditional analysis was applied. Only the following data were retained : prototype data, large-size model data ($h > 0.020$ m, $Re > 1E+5$), and model studies published after January 1997. This analysis gives a greater statistical weight to prototype data and recent works. Basic results of the conditional analysis indicate different trends for flat and steep chutes (Fig. 4A & 4B).

For flat chutes ($\theta < 20°$), prototype data obtained with horizontal and downward-inclined steps exhibit higher flow resistance than laboratory data:

[13a] $$\frac{1}{\sqrt{f}} = -1.224 - 1.245 * \text{Ln}\left(\frac{h*\cos\theta}{D_H}\right)$$ for prototype flat chutes

[13b] $$\frac{1}{\sqrt{f_p}} = 2.430 - 0.2676 * \text{Ln}\left(\frac{h*\cos\theta}{D_H}\right)$$ for model flat chutes

with normalised correlation coefficients of 0.9525 (10 data points) and 0.4872 (52 data points) respectively. By comparison, the Colebrook-White formula for flat rough walls is :

[14] $$\frac{1}{\sqrt{f}} = 1.14 - 4.605 * \text{Ln}\left(\frac{k_s'}{D_H}\right)$$

Equation (14) is compared with data and Equation (13) in Figure 4A.

For steep chutes ($\theta > 20°$), the friction factor data present no obvious correlation with the relative step roughness height $h*\cos\theta/D_H$, Reynolds, Froude nor Weber numbers (Fig. 4B). They appear to be distributed around three dominant values : $f \approx 0.105$, 0.17 and 0.30 (166 data points) as shown in Figure 4C.

Discussion

Cavity recirculation and ejection mechanisms

Skimming flows are characterised by unsteady momentum exchanges between the main stream and cavity flows. The recirculating fluid will, at irregular time intervals, be swept away (i.e. flow outward) into the main flow and be replaced by fresh fluid. The ejection mechanism appears sequential. Once one cavity outflow occurs, it induces a sequence of outflows at the downstream cavities. The sequential process is illustrated in Figure 5. The sequential ejection process extends down the entire slope. It was observed visually for all investigated slopes by Yasuda and Ohtsu (1999) and Chanson and Toombes (2001a), but the sequential mechanism seemed more frequent on the steep chute geometries. A similar pattern was documented with skimming flows past strip roughness (Rectangular cavity: Djenidi et al. 1994, Elavarasan et al. 1995; Triangular cavity: Tantirige et al. 1994) while the sequential fluid ejection process was observed on the M'Bali stepped spillway model by Professor Lejeune.

Cavity recirculation is very energetic and contributes significantly to the form drag. Turbulent motion in the step cavity induces viscous dissipation while irregular fluid exchanges with the free-stream maintain the recirculation process. Energy considerations provide a relationship between cavity ejection frequency, form drag and energy dissipation.

At uniform equilibrium, the rate of energy loss between two adjacent step edges equals ρ_w*Q_w*h, while the energy is dissipated in the recirculation cavity at a rate proportional to the ejection frequency F_{ej}, the volume of ejected fluid and the main flow velocity V. The energy principle yields an analytical relationship between the dimensionless fluid ejection frequency and rate of energy loss which may expressed in terms the dimensionless shear stress:

[15] $$\frac{F_{ej} * (h*\cos\theta)}{V} \approx \frac{f}{5}$$

where F_{ej} is the average fluid ejection frequency. Equation (15) was derived for a wide chute with horizontal steps assuming that the ratio of average fluid ejection volume to total cavity volume is about 0.5 (Chanson and Toombes 2001b, pp. 56-58) and that the ratio of average ejection period to burst duration is about 7 (Djenidi et al. 1994, Tantirige et al. 1994). Note that, according to linear stability theory for a convective-type instability, a higher order cavity flow frequency is related to the flow momentum thickness and velocity (Lin and Rockwell 2001).

The result (Eq. (15)) has practical applications in terms of fluid-structure interactions because cavity oscillations are the origin of coherent, broad-band sources of noise as well as flow-induced vibrations. For example, if the natural frequency of the spillway structure equal F_{ej}, major vibrations may occur leading to potential damage and failure. Equation (15) suggests further that flow visualisations of cavity ejections and cavity pressure fluctuation measurements may provide some information on the flow resistance.

Interactions between the turbulent free-stream and unsteady recirculating flow are driven by the shear layer impingement process at the downstream end of the cavity (Fig. 1). In turn, the upstream flow conditions might affect self-excited cavity oscillations, inducing alterations of the mean drag (e.g. Lin and Rockwell 2001). Chanson and Toombes (2001b, pp. 36-38) suggested that different values of equivalent form drag friction factor might be related to different types of upstream flow conditions : i.e., f = 0.105, 0.17 and 0.30 in Figure 4C.

Flow resistance on flat slopes

For flat slopes ($\theta < 20°$), the results highlight some discrepancy between model and prototype data which remains unexplained (Fig. 4A). However it must be noted that the Brushes Clough spillway data were obtained for flow conditions characterised by Froude numbers close to unity (Fr ~ 0.6 to 1.2) and at the upper limit of the transition to skimming flow regimes (i.e. $d_c/h \sim 0.8$ to 1). The Dneiper power plant data were obtained in decelerating flow conditions with Froude numbers slightly greater than unity (Fr ~ 1.2 to 4). In laboratory, larger Froude number (Fr ~ 3.3 to 5) were observed. Although it is acknowledged that the prototype data might not be truly representative, these full-scale data exhibit some consistency between two series of experiments performed independently (i.e. Brushes Clough in UK and Dneiper in Ukraine).

In practice, it is believed that Equation (13a) is more representative of prototype flow conditions. The difference between Equations (13a) and (13b) could suggest some form of scale effects. On flat slope, the free-surface is not parallel to the pseudo-bottom but it exhibits an 'undular' pattern in phase with the step geometry. The flow resistance is a combination of form drag and skin friction on the downstream end of each step. The interactions of the developing shear layer onto the downstream step are significant, and the process may not be scaled properly with a Froude similitude. Further prototype flows were characterised by a larger Reynolds number and a larger relative channel width B/d than model experiments. It is possible that the three-dimensional recirculation vortices were more intense, leading to larger flow resistance data.

Flow resistance on steep slopes

For steep slopes ($\theta > 20°$), there is no skin friction between the main flow and the step faces, and the form drag associated with the recirculation predominates. The cavity flow is three-dimensional as visually observed during the present study, by Matos et al. (1999) and by Lejeune on the M'Bali model. The flow resistance is a function of the recirculation process and energy dissipation is dominated by the transfer of momentum between the cavity flow and the main stream. A simplified theoretical model (App. I) suggests that the pseudo-boundary shear stress form drag f_d may be expressed, in dimensionless form, as :

$$[16] \quad f_d = \frac{2}{\sqrt{\pi}} * \frac{1}{K}$$

where 1/K is the dimensionless rate of expansion of the shear layer (Fig. 1). In air-water mixing layers, Brattberg and Chanson (1998) observed K ~ 6 for V = 2 to 8 m/s. Equation (16) predicts f_d about 0.2 for a steep chute skimming flow which is close to the observed friction factor in skimming flow. Equation (6) is shown in Figure 4B.

For steep slopes, the reasonable agreement between all the model data and the analytical development (Eq. (16)) suggests that the analysis criteria (i.e. h > 0.020 m & Re > 1E+5) are satisfactory requirements for physical modelling of flow resistance in skimming flows based upon a Froude similitude using a geometric similarity and same fluids (air & water) in model and prototype. A further condition exists to achieve true similarity of air entrainment : i.e., a model scale between 1/1 to 1/10 (Esslingen 1984, Chanson 1997).

In Figure 4B, the flow resistance data based upon detailed air-water flow measurements appear centred around f_e ~ 0.15. The data account however for any drag reduction induced by free-surface aeration (Chanson 1993). For design purposes, Equation (16) may provide a satisfactory estimate of the flow resistance : i.e., $f_e = f_d = 0.2$.

Final remarks

It is believed that the channel width does affect the development and number of recirculating cells at each step. For steep chutes ($\theta > 20°$), data from Chamani and Rajaratnam (1999) and Yasuda and Ohtsu (1999) suggest slightly higher friction factors for low aspect ratios (i.e. $W/h \le 10$) with identical flow conditions and geometry. Note that both studies used a constant channel breadth, W = 0.3 and 0.4 m respectively, and the effect of the channel width was not specifically investigated.

Lastly flat slope prototype data exhibit greater friction factors than all model data while laboratory data show flow resistance estimate nearly independent of the slope.

Conclusion

In skimming flows down stepped chutes, the external edges of the steps form a pseudo-bottom over which the flow passes. Beneath this, recirculating vortices develop and are maintained through the transmission of shear stress from the waters flowing past the step edges. Skimming flows are characterised by a large flow resistance which is caused by form losses. The flow resistance is consistently larger than on smooth-invert channels. Unsteady interactions between the recirculating cavities and the main stream are important. Flow visualisations suggest irregular fluid ejections from the cavity into the main stream, the process being sequential from upstream to downstream. On flat chutes ($\theta < 20°$), the flow resistance is a combination of skin friction on the horizontal faces of the steps and form drag associated with the recirculating cavity. The flow resistance data may differ from steep chute data and they may be correlated with the relative step roughness. Prototype results may be estimated by Equation (13a) but further work is required to understand the difference between model and prototype data.

On steep chutes (θ > 20º), the flow resistance must be analysed as a form drag. It may be estimated from the maximum shear stress in the shear layers: Equation (16) presents a simple model of form loss that agrees well with steep chute data. Although they exhibit some scatter, the data are distributed around three dominant values (f ~ 0.1, 0.17 and 0.30). Air-water flow data show smaller estimate $f_e \sim 0.15$, but the results may take into account some drag reduction induced by free-surface aeration. Physical modelling of flow resistance may be conducted based upon a Froude similitude provided that the laboratory conditions satisfy h > 0.020 m and Re > 1E+5. To achieve true similarity of air entrainment, the model scale must be between 1/1 to 1/10.

The study emphasises the complexity of skimming flow on stepped chutes and the effects of free-surface aeration cannot be neglected. The flow resistance and energy dissipation processes are dominated by form losses and cavity recirculation.

Acknowledgments

The authors thank a large number of people for providing their experimental data, including Dr R. Baker, Univ. of Salford, UK, Dr J. Matos, IST-Lisbon, Portugal, Mr P. Royet, CEMAGREF and Dr L. Toombes, Univ. of Queensland, Australia. The first author acknowledges the helpful discussion with Professor C.J. Apelt, University of Queensland, Australia and Professor A. Lejeune, University of Liège, Belgium.

Appendix - Modelling form drag and flow resistance in skimming flows

Skimming flows are characterised by unsteady momentum exchanges between the main stream and cavity flows. For steep slope (θ > 20º), the form drag associated with the recirculation is preponderant. The cavity flow is three-dimensional as visually observed by Lejeune on the M'Bali model and during the present study. The flow resistance is a function of the recirculation process and energy dissipation is dominated by the transfer of momentum between the cavity flow and the main stream.

Estimating the boundary shear stress along a recirculating cavity

At each step, the cavity flow is driven by the developing shear layer and the transfer of momentum across it (Fig. 1). The mixing layer is basically a free shear layer. The equivalent boundary shear stress of the cavity flow equals the maximum shear stress in the shear layer that may be modelled by a mixing length model:

$$[\text{A-1}]\quad \frac{V}{V_o} = \frac{1}{2} * \left(1 + \text{erf}\left(\frac{K * (y - y_{50})}{x}\right)\right)$$

assuming a constant eddy viscosity ν_t across the shear layer :

$$[\text{A-2}]\quad \nu_t = \frac{1}{4 * K^2} * x * V_o$$

where 1/K is the dimensionless rate of expansion of the shear layer, y_{50} is the location of the streamline $V = V_o/2$ and V_o is the free-stream velocity (Goertler 1942). The boundary shear stress between the outer flow and the cavity flow equals the maximum shear stress in the mixing layer:

$$[\text{A-3}]\quad \tau_o = \tau_{max} = \rho * \nu_t * \left(\frac{\partial V}{\partial y}\right)_{y=y_{50}}$$

where ν_t is the momentum exchange coefficient (Eq. (A-2)). For Goertler's approximation, the dimensionless pseudo-boundary shear stress equals :

$$[\text{A-4}]\quad f_d = \frac{8 * \tau_{max}}{\rho * V_o^2} = \frac{2}{\sqrt{\pi} * K}$$

where the left handside term is basically a pseudo Darcy friction factor (Chanson et al. 2000).

In air-water mixing layers of plane plunging jets, Brattberg and Chanson (1998) observed K ~ 6 for velocities ranging from 2 to 8 m/s. (For monophase flows, K ~ 12.). Equation (A-4) predicts a form drag: $f_d \approx 0.2$ for skimming flow, a result close to friction factor data in steep stepped flows. In monophase flows, Wygnanski and Fiedler (1970) observed that the maximum shear stress is independent from the distance from the singularity and their data yield f = 0.18. For cavity flows, Haugen and Dhanak (1966) and Kistler and Tan (1967) observed similar results.

Discussion

It must be emphasised that the above development (i.e. Eq. (A-4)) does not take into account the interactions between the developing mixing layer and the downstream step, and the associated losses. Pearson et al. (1997) demonstrated that turbulent flows past a recirculating square cavity are associated with a sharp rise of boundary shear stress downstream of the cavity for up to 6 cavity lengths. Their data showed the magnitude of the shear stress peak being about 3 times the equivalent skin friction stress. They attributed the sharp rise to local intense favourable pressure gradient that is associated with the downstream stagnation edge of the cavity. This is in fact a kind of form drag.

References

BaCaRa 1991. Etude de la Dissipation d'Energie sur les Evacuateurs à Marches. ('Study of the Energy Dissipation on Stepped Spillways.') Rapport d'Essais, Projet National BaCaRa, CEMAGREF-SCP, Aix-en-Provence, France, Oct., 111 pages (in French).

Baker, R. 1994. Brushes Clough Wedge Block Spillway - Progress Report No. 3. SCEL Project Report No. SJ542-4, University of Salford, UK, Nov., 47 pages.

Bayat, H.O. 1991. Stepped Spillway Feasibility Investigation. Proceedings of 17th ICOLD Congress, Vienna, Austria, Q. 66, R. 98, pp. 1803-1817.

Bindo, M., Gautier, J., and Lacroix, F. 1993. The Stepped Spillway of M'Bali Dam. International Water Power and Dam Construction, Vol. 45, No. 1, pp. 35-36.

Boes, R.M. 2000. Zweiphasenstroömung und Energieumsetzung auf Grosskaskaden. Ph.D. thesis, VAW-ETH, Zürich, Switzerland.

Brattberg, T., and Chanson, H. 1998. Air Entrapment and Air Bubble Dispersion at Two-Dimensional Plunging Water Jets. Chemical Engineering Science, Vol. 53, No. 24, Dec., pp. 4113-4127. Errata : 1999, Vol. 54, No. 12, p. 1925.

Chamani, M.R., and Rajaratnam, N. 1999. Characteristics of Skimming Flow over Stepped Spillways. Journal of Hydraulic Engineering, ASCE, Vol. 125, No. 4, pp. 361-368.

Chanson, H. 1993. Stepped Spillway Flows and Air Entrainment. Canadian Journal of Civil Engineering, Vol. 20, No. 3, June, pp. 422-435.

Chanson, H. 1995. Hydraulic Design of Stepped Cascades, Channels, Weirs and Spillways. Pergamon, Oxford, UK.

Chanson, H. 1997. Air Bubble Entrainment in Free-Surface Turbulent Shear Flows. Academic Press, London, UK.

Chanson, H. 1999. The Hydraulics of Open Channel Flows : An Introduction. Edward Arnold, London, UK.

Chanson, H. 2000. Forum article. Hydraulics of Stepped Spillways: Current Status, Journal of Hydraulic Engineering, ASCE, Vol. 126, No. 9, pp. 636-637.

Chanson, H., and Toombes, L. 2001a. Strong Interactions between Free-Surface Aeration and Turbulence down a Staircase Channel. Proceedings of 14th Australasian Fluid Mechanics Conference, Adelaide, Australia, pp. 841-844.

Chanson, H., and Toombes, L. 2001b. Experimental Investigations of Air Entrainment in Transition and Skimming Flows down a Stepped Chute. Application to Embankment Overflow Stepped

Spillways. Research Report CE 158, Dept. of Civil Engineering, University of Queensland, Brisbane, Australia, July, 74 pages.

Chanson, H., Yasuda, Y., and Ohtsu, I. 2000. Flow Resistance in Skimming Flow : a Critical Review. International Workshop on Hydraulics of Stepped Spillways, Zürich, Balkema Publ., pp. 95-102.

Christodoulou, G. C. 1993. Energy Dissipation on Stepped Spillways. Journal of Hydraulic Engineering, ASCE, Vol. 119, No. 5, pp. 644-650. Discussion : Vol. 121, No. 1, pp. 80-87.

Diez-Cascon, J., Blanco, J.L., Revilla, J., and Garcia, R. 1991. Studies on the Hydraulic Behaviour of Stepped Spillways. International Water Power and Dam Construction, Vol. 43, No. 9, Sept., pp. 22-26.

Djenidi, L, Anselmet, F., and Antonia, R.A. 1994. LDA Measurements in a Turbulent Boundary Layer over a D-Type Rough Wall. Experiments in Fluids, Vol. 16, pp. 323-329.

Elavarasan, R., Pearson, B.R., and Antonia, R.E. 1995. Visualization of Near Wall Region in a Turbulent Boundary Layer over Transverse Square Cavities with Different Spacing. Proceedings of 12th Australasian Fluid Mechanics Conference AFMC, Sydney, Australia, Vol. 1, pp. 485-488.

Esslingen 1984. Scale Effects in Modelling Hydraulic StructuResearch Proceedings of International Symp. on Scale Effects in Modelling Hydraulic Structures, IAHR, Esslingen, Germany, H. Kobus editor.

Frizell, K.H. 1992. Hydraulics of Stepped Spillways for RCC Dams and Dam Rehabilitations. Proceedings of 3rd Specialty Conference on Roller Compacted Concrete, ASCE, San Diego CA, USA, pp. 423-439.

Goertler, H. 1942. Berechnung von Aufgaben der freien Turbulenz auf Grund eines neuen Näherungsansatzes. Z.A.M.M., 22, pp. 244-254 (in German).

Grinchuk, A.S., Pravdivets, Y.P., and Shekhtman, N.V. 1977. Test of Earth Slope Revetments Permitting Flow of Water at Large Specific Discharges. Gidrotekhnicheskoe Stroitel'stvo, No. 4, pp. 22-26 (in Russian). (Translated in Hydrotechnical Construction, 1978, Plenum Publ., pp. 367-373).

Haugen, H.L., and Dhanak, A.M. 1966. Momentum Transfer in Turbulent Separated Flow past a Rectangular Cavity. Journal of Applied Mechanics, Trans. ASME, Sept., pp. 641-464.

Henderson, F.M. 1966. Open Channel Flow. MacMillan Company, New York, USA.

Kazemipour, A.K., and Apelt, C.J. 1983. Effects of Irregularity of Form on Energy Losses in Open Channel Flow. Australian Civil Engineering Transactions, I.E.Aust., Vol. CE25, pp. 294-299.

Kistler, A.L., and Tan, F.C. 1967. Some Properties of Turbulent Separated Flows. Physics of Fluids, Vol. 10, No. 9, Pt II, pp. S165-S173.

Knauss, J. 1995. THS GRIAS TO PHDHMA, der Altweibersprung. Die Rätselhafte Alte Talsperre in der Glosses-Schlucht bei Alyzeia in Akarnanien. Archäologischer Anzeiger, Heft 5, pp. 138-162 (in German).

Lin, J.C., and Rockwell, D. 2001. Organized Oscillations of Initially Turbulent Flow past a Cavity. AIAA Journal, Vol. 39, No. 6, pp. 1139-1151.

Matos, J. 2000. Hydraulic Design of Stepped Spillways over RCC Dams. International Workshop on Hydraulics of Stepped Spillways, Zürich, Balkema Publ., pp. 187-194.

Matos, J., Sanchez, M., Quintela, A., and Dolz, J. 1999. Characteristic Depth and Pressure Profiles in Skimming Flow over Stepped Spillways. Proceedings of 28th IAHR Congress, Graz, Austria, Session B14 (CD-ROM).

Nihon University 1998. Hydraulic Characteristics of Stepped Channel Flows. Workshop on Flow Characteristics around Hydraulic Structures and River Environment, University Research Center, Nihon University, Tokyo, Japan, November, Edited by I. Ohtsu and Y. Yasuda, 55 pages.

Ohtsu, I., and Yasuda, Y. 1997. Characteristics of Flow Conditions on Stepped Channels. Proceedings of 27th IAHR Biennal Congress, San Francisco, USA, Theme D, pp. 583-588.

Ohtsu, I, Yasuda, Y., and Takahashi, M. 2000. Characteristics of Skimming Flow over Stepped Spillways. Discussion. Journal of Hydraulic Engineering, ASCE, Vol. 126, No. 11, pp. 869-871.

Pearson, B.R., Elavarasan, R., and Antonia, R.A. 1997. The Response of a Turbulent Boundary Layer to a Square Groove. Journal of Fluids Engineering, Trans. ASME, Vol. 119, June, pp. 466-469.

Peyras, L., Royet, P., and Degoutte, G. 1991. Ecoulement et Dissipation sur les Déversoirs en Gradins de Gabions. ('Flows and Dissipation of Energy on Gabion Weirs.') Journal La Houille Blanche, No. 1, pp. 37-47 (in French).

Ruff, J.F., and Frizell, K.H. 1994. Air Concentration Measurements in Highly-Turbulent Flow on a Steeply-Sloping Chute. Proceedings of Hydraulic Engineering Conference, ASCE, Buffalo, USA, Vol. 2, pp. 999-1003.

Schlichting, H. 1979. Boundary Layer Theory. McGraw-Hill, New York, USA, 7th edition.

Shvajnshtejn, A.M. 1999. Stepped Spillways and Energy Dissipation. Gidrotekhnicheskoe Stroitel'stvo, No. 5, pp. 15-21 (in Russian). (Also Hydrotechnical Construction, Vol. 3, No. 5, 1999, pp. 275-282.)

Sorensen, R.M. 1985. Stepped Spillway Hydraulic Model Investigation. Journal of Hydraulic Engineering, ASCE, Vol. 111, No. 12, pp. 1461-1472. Discussion : Vol. 113, No. 8, pp. 1095-1097.

Tantirige, S.C., Iribarne, A.P., Ojhas, M., and Trass, O. 1994. The Turbulent Boundary Layer over Single V-shaped Cavities. International Journal Heat Mass Transfer, Vol. 37, pp. 2261-2271.

Tozzi, M., Taniguchi, E., and Ota, J. 1998. Air Concentration in Flows over Stepped Spillways. Proc. 1998 ASME Fluids Engineering Conference, FEDSM'98, Washington DC, USA, June 21-25, Paper FEDSM98-5053, 7 pages (CD-ROM).

Wygnanski, I., and Fiedler, H.E. 1970. The Two-Dimensional Mixing Region. Journal of Fluid Mechanics, Vol. 41, Part 2, pp. 327-361.

CHANSON, H., YASUDA, Y., and OHTSU, I. (2002). "Flow Resistance in Skimming Flows and its Modelling." *Can Jl of Civ. Eng.*, Vol. 29, No. 6, pp. 809-819 (ISSN 0315-1468).

Yasuda, Y., and Ohtsu, I. 1999. Flow Resistance of Skimming Flow in Stepped Channels. Proceedings of 28th IAHR Congress, Graz, Austria, Session B14, 6 pages (CD-ROM).

List of symbols

A_w	cross-section area (m^2) of the water flow;
C	air concentration defined as the volume of air per unit volume;
	(Note : it is also called void fraction);
C_{mean}	depth averaged air concentration defined as : $(1 - Y_{90}) * C_{mean} = d$;
C_P	pressure correction coefficient;
D_H	hydraulic diameter (m);
D'	dimensionless air bubble diffusivity;
d	1- flow depth measured normal to the channel slope at the edge of a step;
	2- characteristic depth (m) defined as : $d = \int_0^{Y_{90}} (1 - C) *dy$;
d_1	flow depth (m) upstream of a hydraulic jump;
d_2	flow depth (m) downstream of a hydraulic jump;
F_{ej}	average fluid ejection frequency (Hz);
Fr	Froude number defined as : $Fr = V/\sqrt{g*d}$;
f	Darcy friction factor;
f_w	Darcy friction factor for clear-water (non-aerated) flow;
f_d	(equivalent) Darcy friction factor estimate of the form drag;
f_e	Darcy friction factor for air-water flow;
f_p	Darcy friction factor calculated using Equation (12);
g	gravity constant (m/s^2) or acceleration of gravity;
H	total head (m);
H_{res}	residual head (m) at the downstream end of the chute;
h	height of steps (m) (measured vertically);
K	inverse of the spreading rate of a turbulent shear layer;
K'	integration constant (defined by Chanson 1997);
k_s	step dimension (m) measured normal to the flow direction : $k_s = h * \cos\alpha$;
k_s'	surface (skin) roughness height (m);
l	horizontal length of steps (m) (measured perpendicular to the vertical direction);
P	pressure (Pa);
P_{bottom}	invert pressure (Pa);
P_w	wetted perimeter (m);
q	discharge per unit width (m^2/s);
Re	Reynolds number defined as : $Re = V*D_H/\nu_w$;
S_f	friction slope : $S_f = - \partial H/\partial x$;

V	clear-water flow velocity (m/s) : $V = q_w/d = q_w / \int_0^{Y_{90}} (1 - C) * dy$;
V_o	free-stream velocity (m/s);
V_1	flow velocity (m/s) upstream of a hydraulic jump;
V_2	flow velocity (m/s) downstream of a hydraulic jump;
v	local velocity (m/s);
W	channel width (m);
x	longitudinal distance (m) measured in the flow direction;
Y_{90}	characteristic depth (m) where the air concentration is 90%;
y	distance (m) from the pseudo-bottom (formed by the step edges) measured perpendicular to the flow direction;
y_{50}	distance (m) normal to the invert where $V = V_o/2$;

Greek symbols

μ	dynamic viscosity (N.s/m^2);
ν	kinematic viscosity (m^2/s);
ν_t	turbulent kinematic viscosity (m^2/s);
θ	channel slope;
ρ	density (kg/m^3);
σ	surface tension between air and water (N/m);
τ	shear stress (Pa);
τ_{max}	maximum shear stress (Pa) in a shear layer;
τ_o	average bottom shear stress (Pa);

Subscript

c	critical flow conditions;
w	water flow;

Abbreviations

RCC roller compacted concrete.

Table 1 - Re-analysed experimental data of flow resistance in skimming flows

Analysis (1)	Reference (2)	Details (3)

f_e	Baker (1994)	Brushes Clough dam spillway. Inclined downwards steps. θ = 18.4º, h = 0.19 m. Trapezoidal channel.
	Ruff and Frizell (1994)	Inclined downwards steps. θ = 26.6º, h = 0.154 m, W = 1.52 m.
	Chamani and Rajaratnam (1999)	θ = 51.3º, h = 0.313, 0.125 m, W = 0.3 m. θ = 59º, h = 0.313 to 0.125 m, W = 0.3 m.
	Ohtsu et al. (2000)	θ = 55º, h = 0.025 m, W = 0.4 m.
	Matos (2000)	θ = 53.1º, h = 0.08 m, W = 1.0 m.
	Boes (2000)	θ = 30º, h = 0.046, 0.092 m, W = 0.5 m. θ = 50º, h = 0.031, 0.093 m, W = 0.5 m.
	Chanson and Toombes (2001a)	θ = 15.9º, h = 0.05, 0.10 m, W = 1 m. θ = 21.8º, h = 0.10 m, W = 1 m.
f_w	Grinchuk et al. (1977)	Dneiper power plant. θ = 8.7º, h = 0.41 m, W = 14.2 m.
	BaCaRa (1991)	θ = 53.1º, h = 0.06 m, W = 1.5 m. θ = 53.1º, h = 0.024 m. θ = 59º, h = 0.024 m. θ = 63.4º, h = 0.024 m.
	Bayat (1991)	θ = 51.3º, h = 0.02 to 0.03 m, W = 0.3 m.
	Bindo et al. (1993)	θ = 51.3º, h = 0.019 and 0.038 m, W = 0.9 m.
	Christodoulou (1993)	θ = 55º, h = 0.025 m, W = 0.5 m.
	Diez-Cascon et al. (1991)	θ = 53.1º, h = 0.03 & 0.06 m, W = 0.8 m.
	Frizell (1992)	Inclined downwards steps. θ = 26.6º, h = 0.051 m, W = 0.457 m.
	Peyras et al. (1991)	Gabion models. θ = 18.4, 26.6 & 45º, h = 0.02 m, W = 0.8 m.
	Shvajnshtejn (1999)	θ = 38.7º, h = 0.05 m, W = 0.48 m. θ = 51.3º, h = 0.0625 m, W = 0.48 m.
	Sorensen (1985)	θ = 52º, h = 0.0024 & 0.061 m, W = 0.305 m.
f_p	Yasuda and Ohtsu (1999)	θ = 5.7º, h = 0.006 to 0.010 m, W = 0.4 m. θ = 11.3º, h = 0.006 to 0.10 m, W = 0.4 m. θ = 19º, h = 0.002 to 0.08 m, W = 0.4 m. θ = 30º, h = 0.004 to 0.07 m, W = 0.4 m. θ = 55º, h = 0.003 to 0.064 m, W = 0.4 m.

<u>List of captions</u>

Fig. 1 - Skimming flow - Definition sketch

Fig. 2 - Darcy friction factor of skimming flows on steep stepped chute (θ > 20º) {455 laboratory data}

Fig. 3 - Void fraction distributions in stepped chute flows : comparison with Equation (6)

CHANSON, H., YASUDA, Y., and OHTSU, I. (2002). "Flow Resistance in Skimming Flows and its Modelling." *Can Jl of Civ. Eng.*, Vol. 29, No. 6, pp. 809-819 (ISSN 0315-1468).

Fig. 4 - Flow resistance in skimming flow : conditional analysis

(A) Flat stepped chute data (θ < 20 deg.) {62 data} - Comparison with Equations (13a) and (13b)

(B) Steep stepped chute data (θ > 20 deg.) {166 data} - Comparison with Equation (16)

(C) Probability distribution function of steep chute friction factor (θ > 20 deg.) {166 data}

Fig. 5 - Sketch of sequential fluid ejections in skimming flows

CHANSON, H., YASUDA, Y., and OHTSU, I. (2002). "Flow Resistance in Skimming Flows and its Modelling." *Can Jl of Civ. Eng.*, Vol. 29, No. 6, pp. 809-819 (ISSN 0315-1468).

Fig. 1 - Skimming flow - Definition sketch

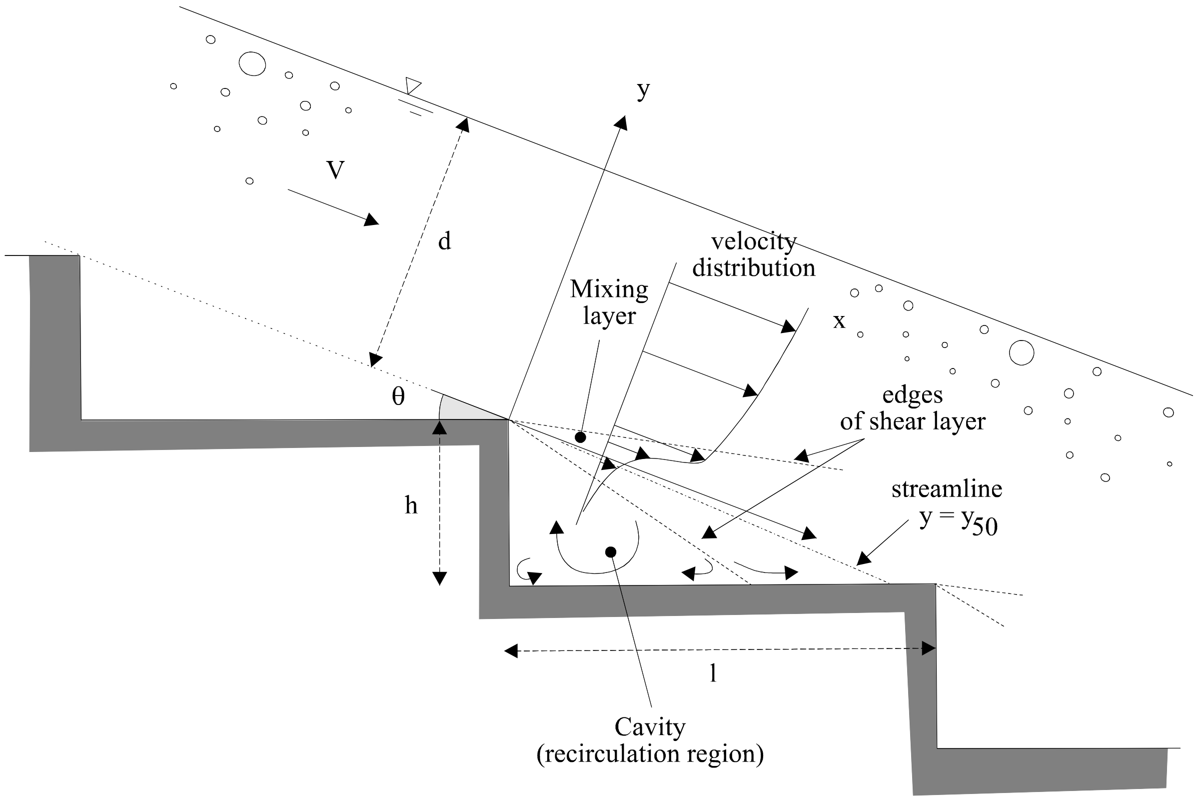

CHANSON, H., YASUDA, Y., and OHTSU, I. (2002). "Flow Resistance in Skimming Flows and its Modelling." *Can Jl of Civ. Eng.*, Vol. 29, No. 6, pp. 809-819 (ISSN 0315-1468).

Fig. 2 - Darcy friction factor of skimming flows on steep stepped chute (θ > 20º) {455 laboratory data}

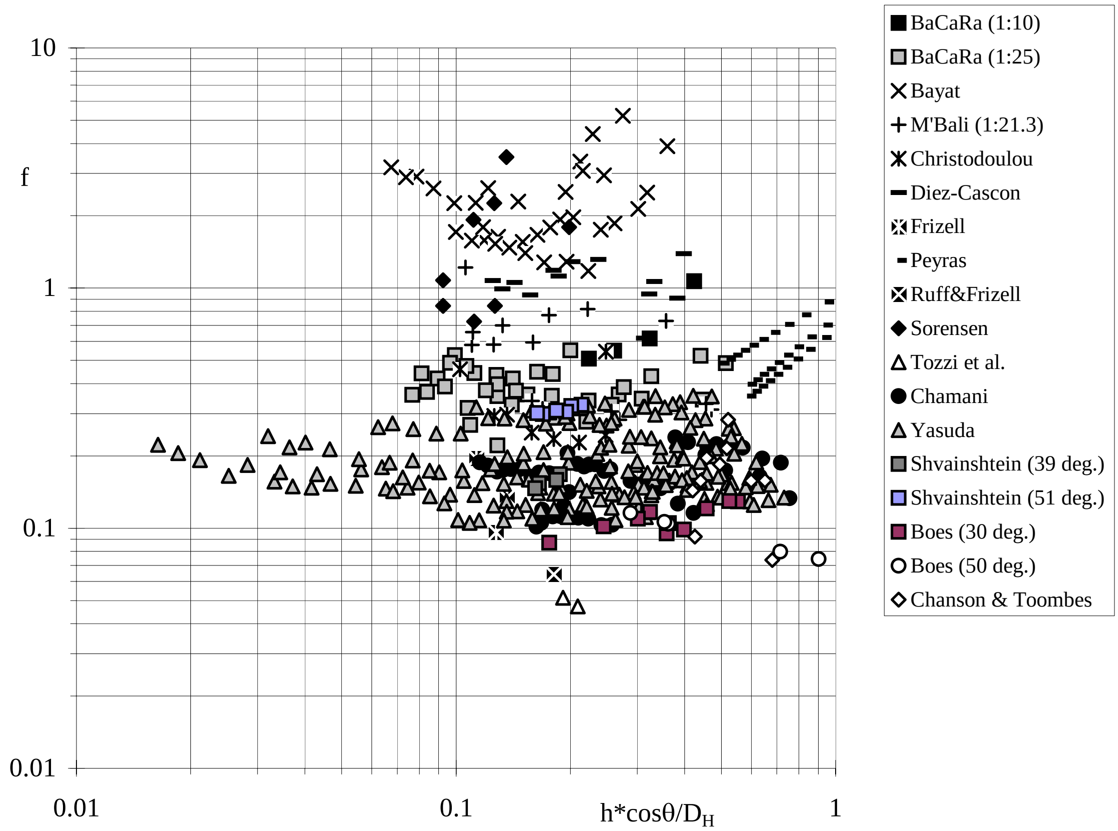

CHANSON, H., YASUDA, Y., and OHTSU, I. (2002). "Flow Resistance in Skimming Flows and its Modelling." *Can Jl of Civ. Eng.*, Vol. 29, No. 6, pp. 809-819 (ISSN 0315-1468).

Fig. 3 - Void fraction distributions in stepped chute flows : comparison with Equation (6)

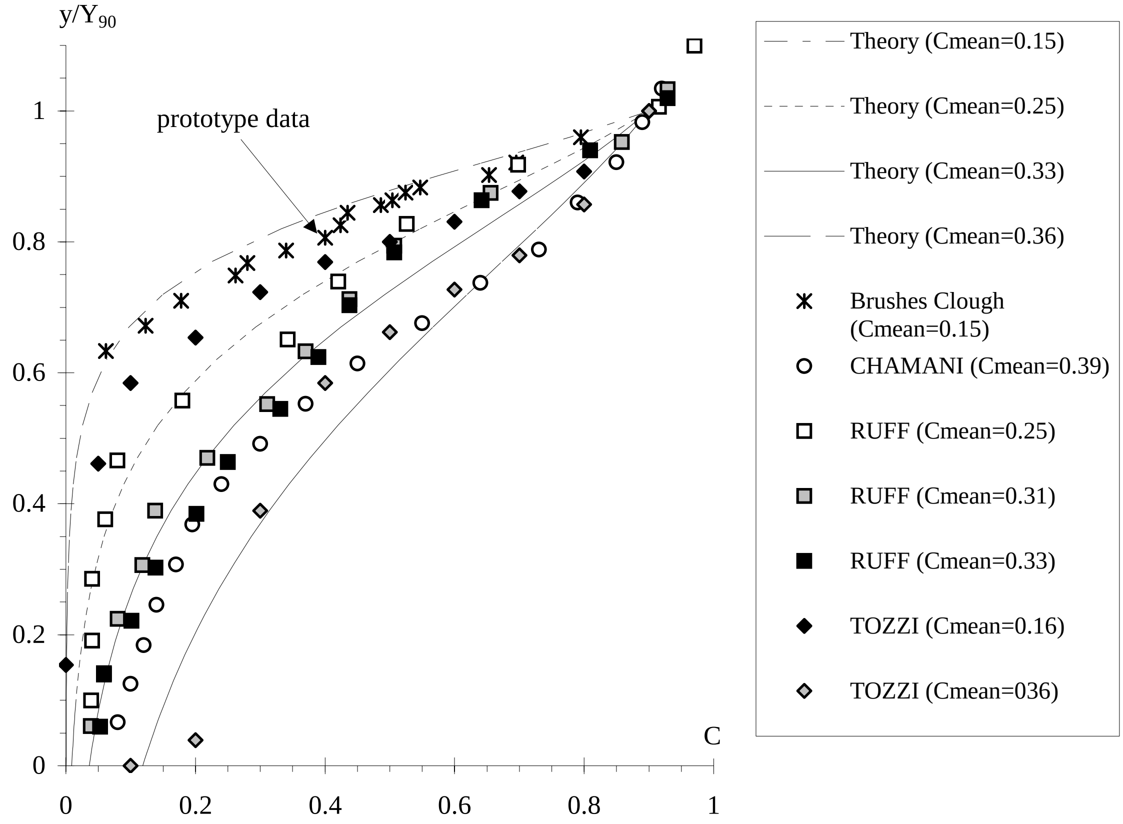

CHANSON, H., YASUDA, Y., and OHTSU, I. (2002). "Flow Resistance in Skimming Flows and its Modelling." *Can Jl of Civ. Eng.*, Vol. 29, No. 6, pp. 809-819 (ISSN 0315-1468).

Fig. 4 - Flow resistance in skimming flow : conditional analysis

(A)

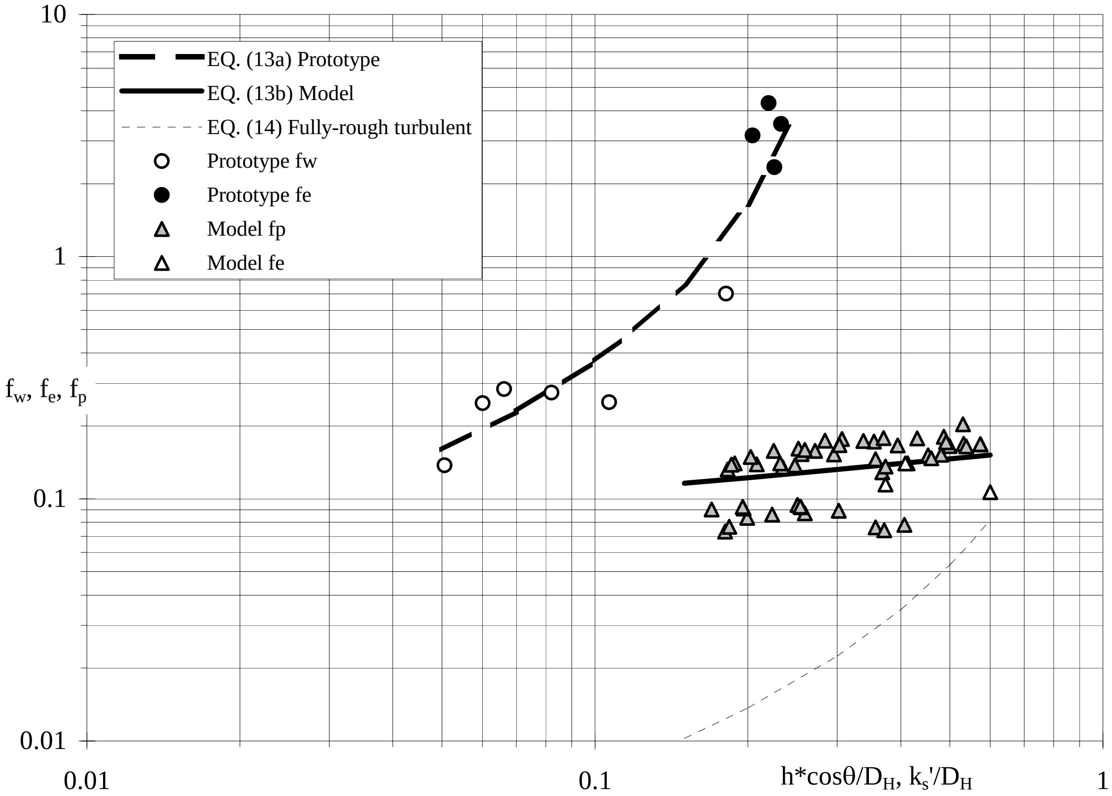

(B)

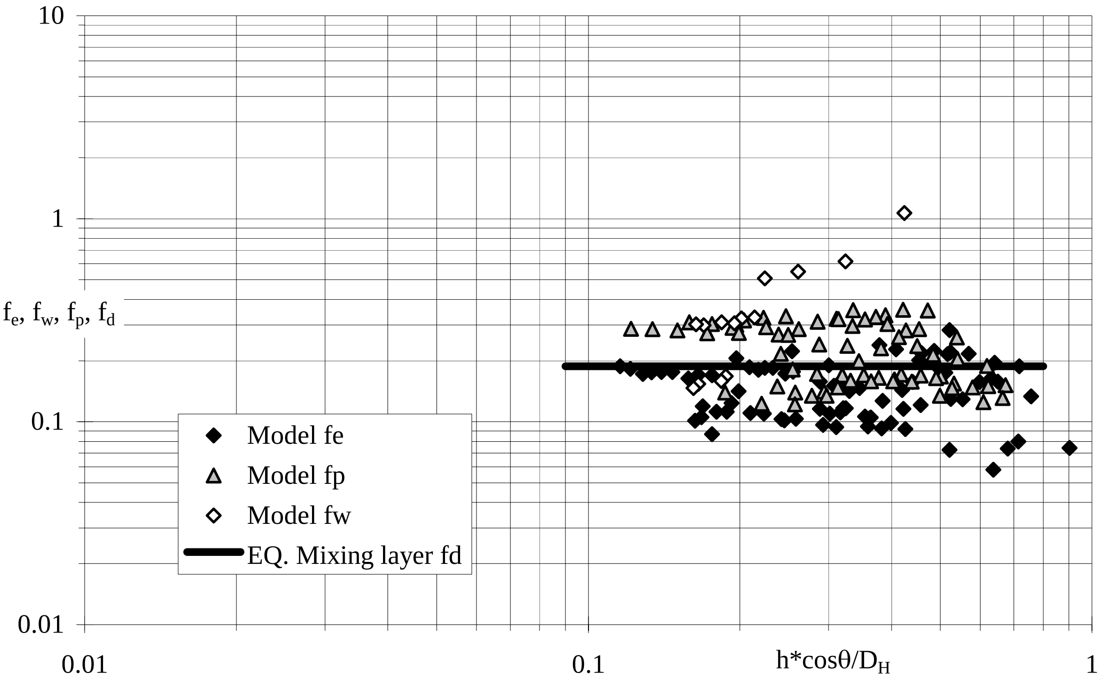
10
1
0.1
0.01
f_e, f_w, f_p, f_d
0.01
0.1
1
h*cosθ/D_H
Model fe
Model fp
Model fw
EQ. Mixing layer fd

(C)

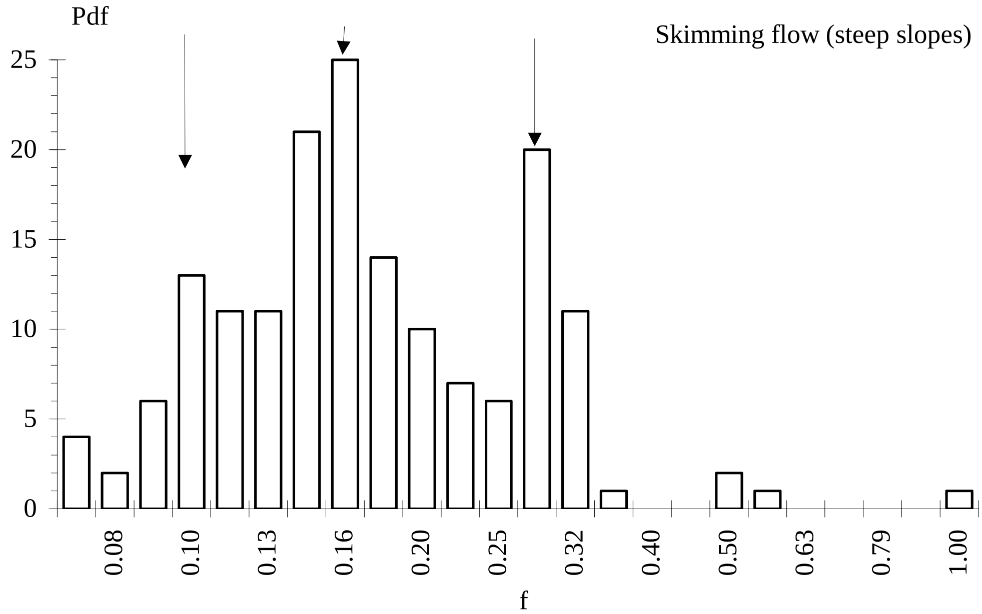
Pdf
Skimming flow (steep slopes)
25
20
15
10
5
0
0.08
0.10
0.13
0.16
0.20
0.25
0.32
0.40
0.50
0.63
0.79
1.00
f

CHANSON, H., YASUDA, Y., and OHTSU, I. (2002). "Flow Resistance in Skimming Flows and its Modelling." *Can Jl of Civ. Eng.*, Vol. 29, No. 6, pp. 809-819 (ISSN 0315-1468).

Fig. 5 - Sketch of sequential fluid ejections in skimming flows